Journal of Organometallic Chemistry 694 (2009) 4014–4024

Contents lists available at ScienceDirect

Journal of Organometallic Chemistry

journal homepage: www.elsevier.com/locate/jorganchem

Palladium acetate complexes bearing chelating *N*-heterocyclic carbene (NHC) ligands: Synthesis and catalytic oxidative homocoupling of terminal alkynes

Tsun-Hung Hsiao [a], Tzu-Liang Wu [a], Sandipan Chatterjee [a], Chin-Yi Chiu [a], Hon Man Lee [a,*], Lorenzo Bettucci [b], Claudio Bianchini [b], Werner Oberhauser [b,*]

[a] Department of Chemistry, National Changhua University of Education, Changhua 50058, Taiwan
[b] Istituto di Chimica dei Composti Organometallici (ICCOM-CNR), Area di Ricerca, CNR di Firenze, Via Madonna del Piano 10, 50019 Sesto Fiorentino, Italy

ARTICLE INFO

Article history:
Received 29 July 2009
Received in revised form 24 August 2009
Accepted 25 August 2009
Available online 1 September 2009

Keywords:
Oxidative coupling
Terminal alkynes
Palladium
1,3-Diynes

ABSTRACT

The imidazolium salts 1,1′-dibenzyl-3,3′-propylenediimidazolium dichloride and 1,1′-bis(1-naphthalenemethyl)-3,3′-propylenediimidazolium dichloride have been synthesized and transformed into the corresponding bis(NHC) ligands 1,1′-dibenzyl-3,3′-propylenediimidazol-2-ylidene (L_1) and 1,1′-bis(1-naphthalenemethyl)-3,3′-propylenediimidazol-2-ylidene (L_2) that have been employed to stabilize the Pd^{II} complexes $PdCl_2(\kappa^2\text{-}C,C\text{-}L_1)$ (**2a**) and $PdCl_2(\kappa^2\text{-}C,C\text{-}L_2)$ (**2b**). Both latter complexes together with their known homologous counterparts $PdCl_2(\kappa^2\text{-}C,C\text{-}L_3)$ (**1a**) (L_3 = 1,1′-dibenzyl-3,3′-ethylenediimidazol-2-ylidene) and $PdCl_2(\kappa^2\text{-}C,C\text{-}L_4)$ (**1b**) (L_4 = 1,1′-bis(1-naphthalenemethyl)-3,3′-ethylenediimidazol-2-ylidene) have been straightforwardly converted into the corresponding palladium acetate compounds $Pd(\kappa^1\text{-}O\text{-}OAc)_2(\kappa^2\text{-}C,C\text{-}L_3)$ (**3a**) (OAc = acetate), $Pd(\kappa^1\text{-}O\text{-}OAc)_2(\kappa^2\text{-}C,C\text{-}L_4)$ (**3b**), $Pd(\kappa^1\text{-}O\text{-}OAc)_2(\kappa^2\text{-}C,C\text{-}L_1)$ (**4a**), and $Pd(\kappa^1\text{-}O\text{-}OAc)_2(\kappa^2\text{-}C,C\text{-}L_2)$ (**4b**). In addition, the phosphanyl-NHC-modified palladium acetate complex $Pd(\kappa^1\text{-}O\text{-}OAc)_2$ $(\kappa^2\text{-}P,C\text{-}L_5)$ (**6**) (L_5 = 1-((2-diphenylphosphanyl)methylphenyl)-3-methyl-imidazol-2-ylidene) has been synthesized from corresponding palladium iodide complex $PdI_2(\kappa^2\text{-}P,C\text{-}L_5)$ (**5**). The reaction of the former complex with *p*-toluenesulfonic acid (*p*-TsOH) gave the corresponding bis-tosylate complex $Pd(OTs)_2(\kappa^2\text{-}P,C\text{-}L_5)$ (**7**). All new complexes have been characterized by multinuclear NMR spectroscopy and elemental analyses. In addition the solid-state structures of **1b**·DMF, **2b**·2DMF, **3a**, **3b**·DMF, **4a**, **4b**, and **6**·$CHCl_3$·$2H_2O$ have been determined by single crystal X-ray structure analyses. The palladium acetate complexes **3a/b**, **4a/b**, and **6** have been employed to catalyze the oxidative homocoupling reaction of terminal alkynes in acetonitrile chemoselectively yielding the corresponding 1,4-di-substituted 1,3-diyne in the presence of *p*-benzoquinone (BQ). The highest catalytic activity in the presence of BQ has been obtained with **6**, while within the series of palladium-bis(NHC) complexes, **4b**, featured with a *n*-propylene-bridge and the bulky *N*-1-naphthalenemethyl substituents, revealed as the most active compound. Hence, this latter precursor has been employed for analogous coupling reaction carried out in the presence of air pressure instead of BQ, yielding lower substrate conversion when compared to reaction performed in the presence of BQ. The important role of the ancillary ligand acetate in the course of the catalytic coupling reaction has been proved by variable-temperature NMR studies carried out with **6** and **7′** under catalytic reaction conditions.

1. Introduction

Alkyne dimerization, through catalytic oxidative coupling reactions, to give 1,3-diynes is a crucial step in the synthesis of natural [1a] and pharmaceutical products that have antifungal [1b] and antitumor activity [1c]. Furthermore, the polymerization of alkynes gives linear π-conjugated acetylenic oligomers and polymers, that find mainly application as laser dyes, as scintillator, as light-emitting diodes, as piezoelectric and pyroelectric materials [2].

The most applied catalytic oxidative C(sp)–C(sp) coupling reactions of terminal alkynes are Cu-based [3] such as the Glaser- [4], the Cadiot-Chodkiewicz- [3] and the Hay-coupling reaction [5]. The mechanism for these latter coupling reactions is suggested to involve an alkynyldicopper(II) intermediate of the formula $\{Cu_2(\mu\text{-}C{\equiv}CR)_2\}$ which would bring about the formation of 1,3-diynes under the concomitant reduction of copper, that is subsequently reoxidized to Cu^{II}, closing in this way the catalytic cycle [3,6].

* Corresponding authors. Tel.: +886 4 7232105 3523; fax: +886 4 7211190 (H.M. Lee), tel.: +39 055 5225284; fax: +39 055 5225203 (W. Oberhauser).
E-mail addresses: leehm@cc.ncue.edu.tw (H.M. Lee), werner.oberhauser@iccom.cnr.it (W. Oberhauser).

0022-328X/$ - see front matter © 2009 Elsevier B.V. All rights reserved.
doi:10.1016/j.jorganchem.2009.08.039

The application of Pd/Cu-based catalytic systems for the oxidative coupling of terminal alkynes has shown to be performed under notably milder reaction conditions [3] compared to palladium-free catalytic systems, employing a variety of oxidizing agents such as oxygen [7a], air [7b,7c], allylbromide [7d], iodine [7e], bromoacetate [7f], Me_3NO [7g] and chloroacetone [7h] to re-oxidize Pd^0 to Pd^{II}. Also activated alkynes, such as iodoalkynes [8a] and alkynyltriisopropoxyborates [8b] to mention a few, have been employed as substrates in Pd/Cu-based coupling reactions [8,9]. The most employed palladium species for oxidative alkyne coupling reactions bear either triphenylphosphine [7a,7e,7f], chelating diphosphines [7i] or amines [7j] as ligands.

(NHC)-modified palladium compounds and in particular acyclic alkylene-bridged bis(NHC)-modified derivatives [10] have been thoroughly studied by others [11] and us [12]. Most of these palladium complexes were generally employed as precursors for Suzuki- and Heck-type C–C coupling reactions [11a,11c–e,11k,12a], the ethylene–CO copolymerization reactions [11b], the direct C–H activation of methane [11c,11g,11j] and the copper-assisted coupling of terminal alkynes in the presence of an external base [13].

Herein we report the synthesis and characterization of a series of new palladium complexes bearing either chelating bis(NHC) ligands (i.e. **3a/b**, **4a/b**) or a phosphanyl-carbene ligand (i.e. **6** and **7**) (Scheme 1) and their application as catalytic precursors in the copper-free, oxidative-coupling reactions of terminal alkynes, using either *p*-benzoquinone (BQ) or air as oxidizing agent and without the aid of an external base.

2. Results and discussion

2.1. Preparation and characterization of palladium complexes

The synthesis of the ethylene-bridged bis(NHC) ligand precursors, 1,1′-dibenzyl-3,3′-ethylenediimidazolium dichloride and 1,1′-bis(1-naphthalenemethyl)-3,3′-ethylenediimidazolium dichloride, were reported by us previously [12a]. Following a similar synthetic approach, the two new *n*-propylene-bridged bis(NHC) ligand precursors, 1,1′-dibenzyl-3,3′-propylenediimidazolium dichloride and 1,1′-bis(1-naphthalenemethyl)-3,3′-propylenediimidazolium dichloride were prepared in pure forms albeit low yields due to the predominant formation of the monoimidazolium salts. The known precursor dichloropalladium complexes **1a**/**b** were prepared by treating the diimidazolium salts with $Pd(OAc)_2$ [12a]. The analogous complexes **2a**/**b** were similarly obtained in excellent yields (ca. 97%). Both latter complexes exhibit poor solubility in THF and dichloromethane.

The four new palladium acetate complexes with ethylene- (i.e. **3a/b**) and *n*-propylene-bridged carbene ligands (i.e. **4a/b**) were then prepared by the salt metathesis reactions between the corresponding dichloropalladium complex and silver acetate in dichloromethane, obtaining yields in the range of 47–55% (Scheme 2).

All the new complexes are stable in air and towards moisture. They have good solubility in polar solvents, such as chloroform and DMSO. The successful formation of the acetate complexes **3a**/**b** and **4a**/**b** were unambiguously confirmed by ^1H and $^{13}C\{^1H\}$ NMR spectroscopy. The ^1H NMR spectra of **3a**/**b** show four doublets for the ethylene hydrogen atoms, reflecting their diastereotopicity [12a]. In the ^1H NMR spectra of **2a**/**b** and **4a**/**b**, there are two more diastereotopic signals due to an additional CH_2 group. HMBC experiments have been carried out which unambiguously assign the ^1H and the $^{13}C\{^1H\}$ NMR signals of all the diastereotopic groups. Fig. 1 shows the HMBC spectrum of compound **4a**.

The ^1H NMR doublets at 4.96 and 5.97 ppm of **4a** are the diastereotopic benzyl hydrogen atoms that are correlated to the ^{13}C signals for *ipso* phenyl- and carbene carbon atoms at 130.90 and 159.60 ppm, respectively. The identities of both downfield ^{13}C NMR signals at 159.60 and 174.30 ppm were easily assigned, since the former ^{13}C signal correlates with the ^1H doublets assigned to the diastereotopic benzyl hydrogen atoms, whereas the latter ^{13}C signal (i.e. carbonyl group) correlates only with the ^1H NMR signal of the acetate groups.

While the ^{13}C NMR resonances for the carbenic carbons in the *n*-propylene-bridged palladium complexes **2a** and **4a** are shown to be identical, the signal for **4a** shows a slight downfield shift compared to that of its homolog **3a** (i.e. 159.60 (**4a**) versus 156.80 ppm (**3a**)).

Complex **6** was similarly prepared in 85% yield by the salt metathesis reaction between complex **5** [14] and silver acetate (Scheme 3).

Unlike the reactions for **3a**/**b** and **4a**/**b**, the pure compound **6** was obtained only when the reaction was conducted in a 3:1 solvent mixture of dichloromethane and acetonitrile. The reaction between **6** and *p*-TsOH in a 1:1 solvent mixture of dichloromethane and methanol afforded the pure yellow micro-crystalline compound **7** in 75% yield. Compounds **6** and **7** were characterized by multinuclear NMR spectroscopy and elemental analyses. In addition, the solid-state structure of **6** has been determined by a single crystal X-ray structure analysis. The ^1H NMR spectrum of **6** shows two singlets for the methyl hydrogens of the acetate ligands at 1.37 and 1.88 ppm; accordingly, two ^{13}C NMR singlets for the carbonyl carbons at 176.80 and 177.40 ppm have been observed. The carbenic carbon was observed as a doublet at 154.30 ppm with a $^2J_{PC}$ of 11.6 Hz.

Unlike the inequivalence of the ^1H NMR signals for the acetate hydrogens in **6**, **7** shows only one singlet at 2.36 ppm for the methyl hydrogens of the tosylate units. A ^1H NMR spectrum of the latter compound acquired in CH_2Cl_2 at −60 °C showed only a slightly broadening of the ^1H singlet assigned to the tosylate

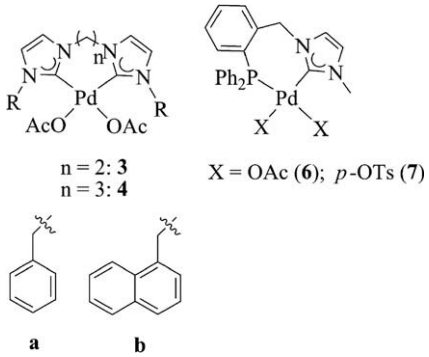

Scheme 1. Synthesized precursors.

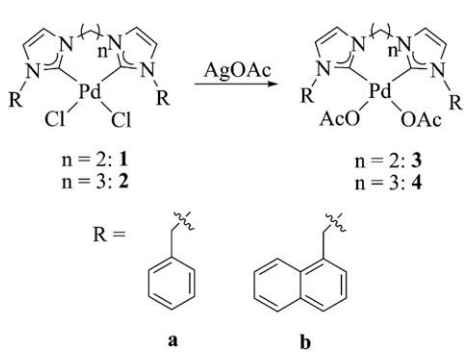

Scheme 2. Synthesis of **3a**/**b** and **4a**/**b**.

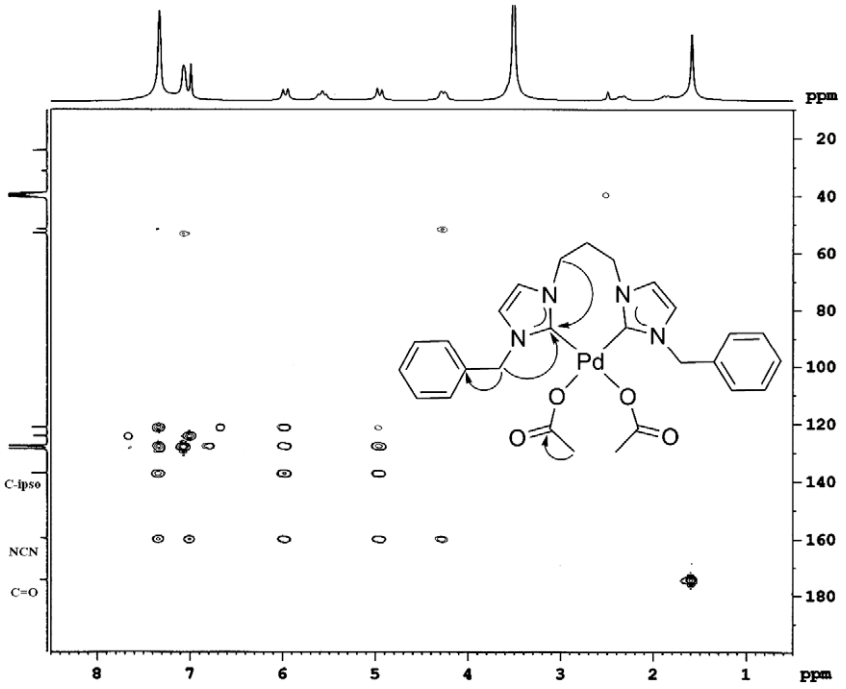

Fig. 1. The HMBC spectrum of **4a** (residual DMSO and its water content are present). The curved arrows indicate the selected HMBC (H → C) described in the text.

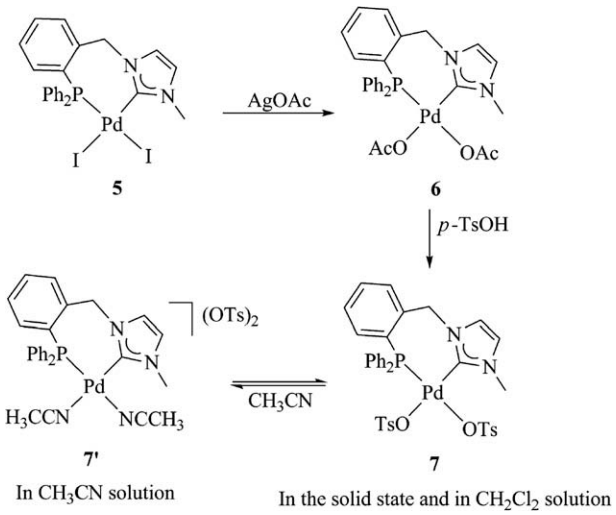

Scheme 3. Synthesis of **6**, **7** and **7′**.

methyl hydrogens, indicating a fluxional behavior of the tosylate anions within the ion pair. Notably, the carbenic carbon at 144.20 ppm in the ^{13}C NMR spectrum of **7** is ca. 10 ppm more upfield than that in the parent compound **6**, which might be rationalized by the weaker *trans*-influence of tosylate compared to acetate and as a consequence the carbene carbon atom in **7** is more strongly coordinated to palladium. It should be further emphasized in this context, that all palladium acetate complexes studied herein behave as non-electrolyte in chloroform, dichloromethane, DMSO, and even in acetonitrile that has been chosen as solvent for the catalytic oxidative coupling reactions. In contrast, the palladium tosylate complex **7** behaves as non-electrolyte in dichloromethane, whereas in acetonitrile both coordinating tosylate moieties are replaced by acetonitrile yielding the bis-cationic compound **7′** (Scheme 3). Importantly, **7′** could not be isolated, since it is stable only in the presence of acetonitrile.

2.2. Crystallographic study

The molecular structures of **1b**·DMF, **2b**·2DMF, **3a**, **3b**·DMF, **4a**/**b**, and **6**·$CHCl_3$·$2H_2O$ were successfully obtained by single crystal X-ray structure analyses. A selected ORTEP plot of each molecular structure is shown in Figs. 2–8. Selected bond lengths and angles

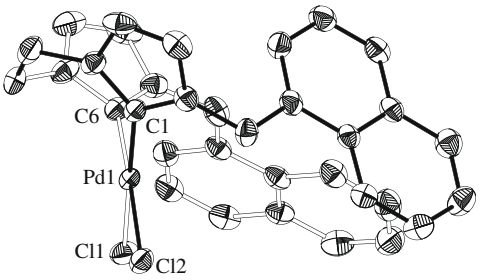

Fig. 2. ORTEP plot of the molecular structure of **1b**·DMF with thermal ellipsoids shown at the 50% probability level. Hydrogen atoms and the solvent molecule are omitted for clarity.

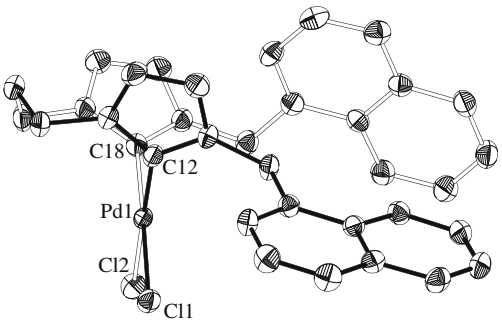

Fig. 3. ORTEP plot of the molecular structure of **2b**·2DMF with thermal ellipsoids shown at the 50% probability level. Hydrogen atoms and solvent molecules are omitted for clarity.

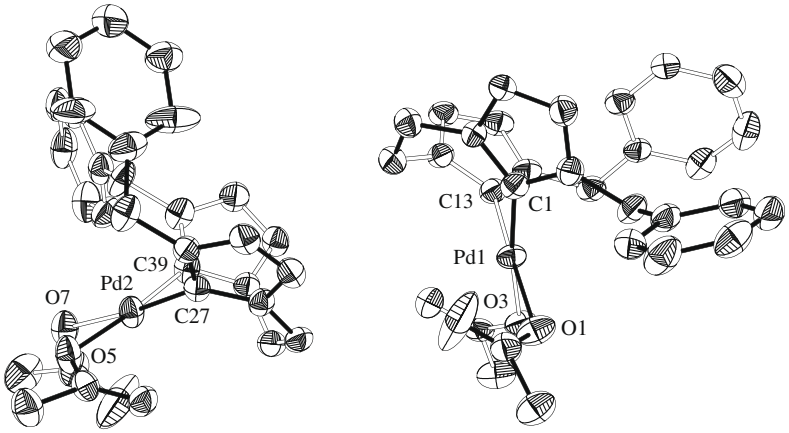

Fig. 4. ORTEP plot of the molecular structure of both conformers of **3a** with thermal ellipsoids shown at the 50% probability level. Hydrogen atoms are omitted for clarity.

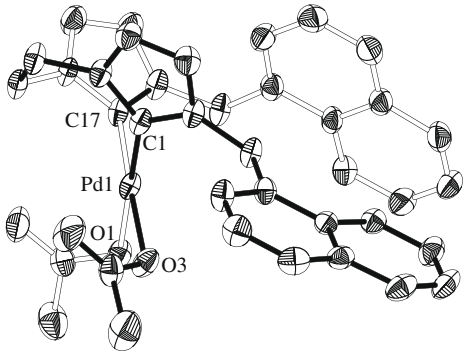

Fig. 5. ORTEP plot of the molecular structure of **3b**·DMF with thermal ellipsoids shown at the 50% probability level. Hydrogen atoms and the solvent molecule are omitted for clarity.

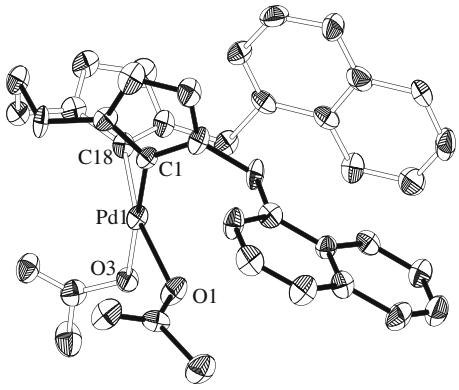

Fig. 7. ORTEP plot of the molecular structure of **4b** with thermal ellipsoids shown at the 50% probability level. Hydrogen atoms are omitted for clarity.

are summarized in Table 1, while crystallographic data are reported in Table 3.

There are two crystallographic independent molecules of **3a**, **4a**, and **6** in their respective asymmetric units. All these palladium complexes show distorted square-planar coordination geometry. The distortion can be inferred by the non-linearity of the two bond angles that involve atoms that are located *trans* to each other with respect to the metal center. Generally, these angles are in the range of 171–179°. However, the C18–Pd1–O1 bond angle in **4b** of 164.8(2)° is exceptionally small. A comparison of the structural parameters of **2b**·2DMF versus **1b**·DMF and of **4a**/**b** versus **3a** and **3b**·DMF reveals that the ligand with a *n*-propylene spacer imposes a larger C–Pd–C bite angle than its ethylene-bridged analog (86.6° in **2b**·2DMF versus 84.6° in **1b**·DMF; 88.0° and 87.1° in **4a** versus 84.4° and 84.1° in **3a**; 88.7° in **4b** versus 83.9° in **3b**·DMF). As expected, the introduction of a C_4-carbon bridge as spacer between imidazol-2-ylidine units leads to an even wider bite angle of ca. 91° as demonstrated in a relevant palladium complex

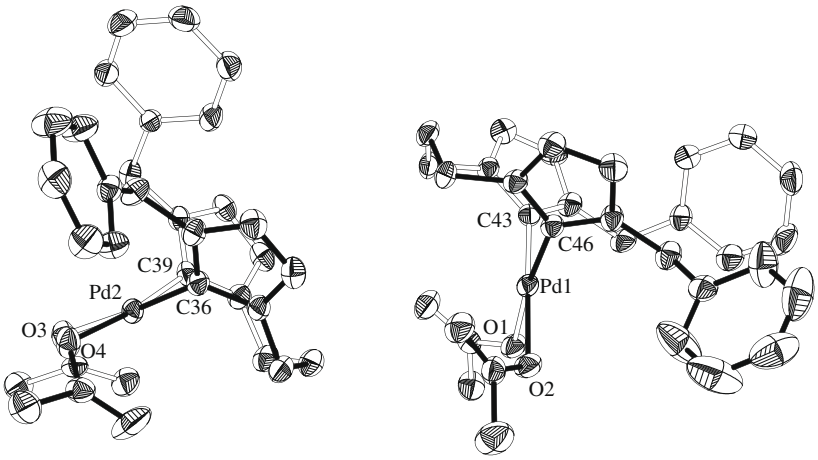

Fig. 6. ORTEP plot of the molecular structure of **4a** with thermal ellipsoids shown at the 50% probability level. Hydrogen atoms are omitted for clarity.

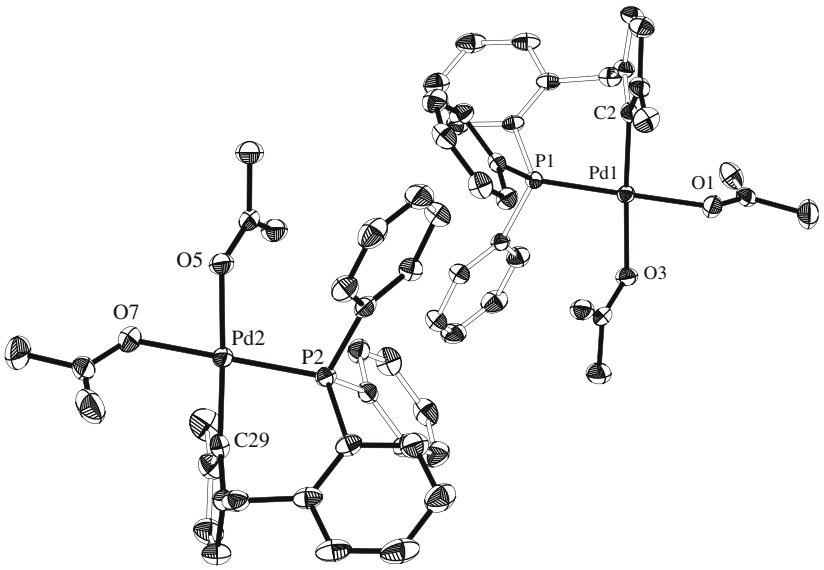

Fig. 8. ORTEP plot of the molecular structure of both conformers of **6**·$CHCl_3$·$2H_2O$ with thermal ellipsoids shown at the 50% probability level. Hydrogen atoms and solvent molecules are omitted for clarity.

[11c]. The seven-membered chelate rings in **1b**·DMF, **3a**, and **3b**·DMF adopt boat conformations with the dihedral angles (α) at 62.7°, 59.6°, and 63.4°, respectively (α = the average angle between the two imidazolium ring planes and the *xy* plane of the metal complex) [15]. Contrastingly, the eight-membered chelate rings in **2b**·2DMF and **4a**/**b** are in boat-chair conformations with larger dihedral angles of 78.3°, 71.3°, and 74.5°, respectively (the O1 atom in **4b** was excluded in the calculation due to its large distortion from the *xy* plane). The chelate ring conformations in these palladium complexes are essentially similar to those of rhodium complexes with similar ligands [15]. The O–Pd–O bond angle in the palladium acetate complexes is comparable to that of reported structures [11h] and significantly smaller when compared to the Cl–Pd–Cl bond angle of the corresponding parent dichloride complex (∠Cl–Pd–Cl = 92.8° in **1b**·DMF versus ∠O–Pd–O = 85.7° in **3b**·DMF; ∠Cl–Pd–Cl = 93.9° in **2b**·2DMF versus ∠O–Pd–O = 87.5° in **4b**). The Pd–carbene carbon bond distances are in the usual range of related compounds in the literature [11c,12a].

The C2–Pd1–P1 bite angles of 86.21(6)° and 85.97(7)° in **6** are slightly larger than that in the complex **5** (84.62(8)°) [14]. Interestingly, the Pd–X bond length (X = I in **5**; O in **6**·$CHCl_3$·H_2O) *trans* to the P-atom is always longer than that *trans* to the carbene moiety (2.6594(3) versus 2.6367(3) Å in **5** [13] and 2.0929(16) and 2.0746(17) versus 2.0607(16) and 2.0671(17) Å in **6**·$CHCl_3$·H_2O), suggesting a larger *trans*-influence exerted by the phosphanyl- than carbene group.

2.3. Catalytic study

Complexes **3a/b**, **4a/b**, **6**, and **7′** were employed as precursors to catalyze oxidative homocoupling reactions of terminal alkynes such as phenylacetylene, 4-ethynyltoluene, and 3,3-dimethyl-1-butyne

Table 1
Selected bond lengths (Å) and angles (°) for **1b**·DMF, **2b**·2DMF, **3a**, **3b**·DMF, **4a**, **4b** and **6**·$CHCl_3$·$2H_2O$.

1b·DMF		**2b**·2DMF		**3a**		**3b**·DMF	
Pd1–Cl1	2.3557(7)	Pd1–Cl1	2.3486(6)	Pd1–O1	2.072(4)	Pd1–O1	2.068(2)
Pd1–Cl2	2.3853(7)	Pd1–Cl2	2.3615(7)	Pd1–O3	2.063(4)	Pd1–O3	2.068(2)
Pd1–C1	1.986(2)	Pd1–C12	1.969(3)	Pd1–C1	1.963(5)	Pd1–C1	1.949(3)
Pd1–C6	1.960(2)	Pd1–C18	1.975(2)	Pd1–C13	1.944(5)	Pd1–C17	1.955(3)
Cl1–Pd1–Cl2	92.80(7)	Cl1–Pd1–Cl2	90.41(7)	Pd2–O5	2.061(4)	O1–Pd1–O3	85.66(7)
C1–Pd1–C6	84.57(19)	C12–Pd1–C18	86.61(10)	Pd2–O7	2.068(4)	C1–Pd1–C17	83.91(10)
				Pd2–C27	1.970(5)		
				Pd2–C39	1.951(5)		
				O1–Pd1–O3	86.00(15)		
				C1–Pd1–C13	84.40(20)		
				O5–Pd2–O7	87.38(15)		
				C27-Pd2–C39	84.10(20)		
4a		**4b**		**6**·$CHCl_3$·$2H_2O$			
Pd1–O1	2.056(2)	Pd1–O1	2.040(4)	Pd1–O1	2.093(2)		
Pd1–O2	2.067(2)	Pd1–O3	2.086(4)	Pd1–O3	2.061(2)		
Pd1–C43	1.966(3)	Pd1–C1	1.966(5)	Pd1–P1	2.2186(6)		
Pd1–C46	1.968(3)	Pd1–C18	1.963(6)	Pd1–C2	1.963(2)		
Pd2–O3	2.056(2)	O1–Pd1–O3	87.47(14)	Pd2–O5	2.067(2)		
Pd2–O4	2.060(2)	C1–Pd1–C18	88.70(20)	Pd2–O7	2.075(2)		
Pd2–C36	1.963(3)			Pd2–P2	2.2202(6)		
Pd2–C39	1.961(3)			Pd2–C29	1.964(2)		
O1–Pd1–O2	85.94(9)			O1–Pd1–O3	86.96(7)		
C43–Pd1–C46	87.97(13)			C2–Pd1–P1	86.21(6)		
O3–Pd2–O4	85.63(9)			O5–Pd2–O7	85.73(7)		
C36–Pd2–C39	87.07(13)			C29–Pd2–P2	85.97(7)		

in acetonitrile, employing BQ or air (i.e. 20 bar) as oxidizing agent. The results obtained from this catalytic study are summarized in Table 2.

Catalytic reactions performed under oxidative conditions afforded the symmetrical 1,4-disubstituted-1,3-diynes chemoselectively (Scheme 4a), while analogous catalytic reactions carried out in the absence of an oxidizing agent (i.e. under a nitrogen atmosphere) yielded only a stoichiometric amount of the 1,3-diyne with respect to the amount of the precursor employed along with trace amounts of the corresponding branched 1,3-enyne (Scheme 4b) (Table 2, entry 7).

A perusal of Table 2 shows that for the oxidative coupling reactions with phenylacetylene carried out in the presence of BQ, **6** was the most efficient precursor, outperforming both reference systems (i.e. [Pd(OAc)$_2$(dppe)] (dppe = 1,2-bis-(diphenylphosphanyl)ethane) [16a] and [Pd(OAc)$_2$(dppp)] (dppp = 1,3-bis-(diphenylphosphanyl)propane) [16b] as well (Table 2, entry 20 versus 27/28). In fact, dppp in combination with $PdCl_2$ and CuI has shown to be an excellent catalytic system for coupling reactions of terminal alkynes [7i]. Within the series of palladium bis(NHC) carbene complexes (i.e. **3a/b** and **4a/b**) tested under identical experimental conditions, **4a/b** featured by bite angles of ca. 87.9° are more active than their homologous compounds **3a/b**, which contain bite angles of ca. 84.1° (entries 5/8 versus 1/3). The same trend of catalytic activity applies for both reference systems (entry 28 versus 27). This experimental finding is in accordance with a positive effect of an increasing ligand bite angle on the rate of the reductive elimination step in catalytic C–C bond formation [17]. The steric congestion of the *N*-substituent of the imidazol-2-ylidene moiety has an opposite effect on the catalytic activity in precursors bearing ethylene-and *n*-propylene-bridged bis-carbene ligands. As a result, precursor **4b**, that combines the 1-methylnaphthyl substitution and the large ligand bite angle leads to the highest catalytic activity (Table 2).

Table 2
Oxidative coupling of terminal alkynes (R-C$_2$H) in acetonitrile employing the precursors **3a**/**b**, **4a**/**b**, **6**, and **7′**.[a]

Entry	Precursor	Substrate (R)-C$_2$H	*t* (h)	Conversion (%)	TOF[b]
1	**3a**	Ph	0.5	24	144
2	**3a**	Ph	1.0	37	111
3	**3b**	Ph	0.5	5	30
4	**3b**	Ph	1.0	8	24
5	**4a**	Ph	0.5	31	186
6	**4a**	Ph	1.0	55	165
7[c]	**4b**	Ph	0.5	2	12
8	**4b**	Ph	0.5	37	222
9	**4b**	Ph	1.0	47	141
10	**4b**	4-Tolyl	0.5	35	210
11	**4b**	4-Tolyl	1.0	43	129
12	**4b**	*ter*-Butyl	2.0	16	24
13	**4b**	*ter*-Butyl	4.0	28	21
14[d]	**4b**	Ph	2.0	28	42
15[d]	**4b**	Ph	4.0	54	41
16[d]	**4b**	4-Tolyl	2.0	20	30
17[d]	**4b**	4-Tolyl	4.0	38	28
18[d]	**4b**	*ter*-Butyl	2.0	12	18
19[d]	**4b**	*ter*-Butyl	4.0	21	16
20	**6**	Ph	0.5	57	342
21	**6**	Ph	1.0	64	192
22	**6**	4-Tolyl	0.5	38	228
23	**6**	4-Tolyl	1.0	47	141
24	**6**	*ter*-Butyl	2.0	9	14
25	**6**	*ter*-Butyl	4.0	16	12
26	**7′**	Ph	0.5	9	54
27	Pd(OAc)$_2$(dppe)	Ph	0.5	23	138
28	Pd(OAc)$_2$(dppp)	Ph	0.5	32	192
29	Pd(OAc)$_2$(dppp)	Ph	1.0	54	162
30[d,e]	Pd(OAc)$_2$/NEt$_3$	Ph	2.0	38	57
31[d,e]	Pd(OAc)$_2$/NEt$_3$	Ph	4.0	60	45

[a] *Catalytic conditions*: precursor, 0.02 mmol; acetonitrile, 25 mL; substrate, 6.0 mmol; BQ, 2.3 mmol; reaction temperature, 70 °C; rpm, 800.
[b] TOF reported as (mmol substrate conv.) × (mmol Pd h)$^{-1}$.
[c] Without oxidizing agent.
[d] Air (20 bar) instead of BQ.
[e] "In situ" synthesized from Pd(OAc)$_2$, 0.02 mmol and NEt$_3$, 0.04 mmol.

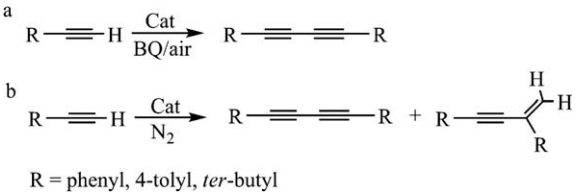

Scheme 4. Organic products obtained from catalytic coupling reactions.

Although **4b** and **6** significantly exhibit deactivation with time (Table 2), both latter precursors proved to be the most active in the oxidative coupling of phenylacetylene and have been therefore employed to catalyze analogous coupling reactions using 4-ethynyltoluene and 3,3-dimethyl-1-butyne as substrates. Regardless of the precursor employed, lower conversions were obtained with these substrates when compared to those observed for phenylacetylene (entries 8 versus 10/12 and 20 versus 22/24). This experimental finding is in agreement with the decreasing Broensted acidity of the corresponding acetylene hydrogen atom on going from phenylacetylene to 3,3-dimethyl-1-butyne. As a result, the rate of the base-assisted formation of the palladium bis-acetylide [3] which is a key species of the oxidative catalytic cycle (Scheme 5, cycle A) decreases in the same order.

The important role of acetate as ancillary ligand has been proven by comparing the catalytic activities between **6** and **7′** under identical experimental conditions (Table 2, entry 20 versus 26). Furthermore variable-temperature NMR studies have been carried out with both precursors under identical catalytic conditions in CD_3CN in the presence of BQ and phenylacetylene. Fig. 9 exhibits a sequence of selected $^{31}P\{^1H\}$ NMR spectra of the variable-temperature NMR study carried out with **6**.

The $^{31}P\{^1H\}$ NMR spectrum of a deaerated solution of **6** in CD_3CN showed at room temperature a singlet at 11.70 ppm (Fig. 9, trace a). On addition of phenylacetylene and BQ to the solution, the signal vanished completely (Fig. 9, trace b). A ^1H NMR spectrum acquired at room temperature proved the beginning of the catalytic process. On heating the NMR probe to 50 °C, the $^{31}P\{^1H\}$ NMR spectrum showed the reappearance of **6** (trace c). Further heating of the reaction mixture to 70 °C led to an increase in intensity of the signal (trace d), while the corresponding ^1H NMR spectrum at 70 °C and a GC–MS analysis at room temperature confirmed the completeness of the substrate conversion.

A parallel low-temperature $^{31}P\{^1H\}$ NMR experiment carried out at −40 °C with an NMR solution identical to that used for the acquisition of the $^{31}P\{^1H\}$ spectrum as reported in Fig. 9 (trace b), showed several singlets in the chemical shift range from −2.1 to 9.2 ppm.

A variable-temperature $^{31}P\{^1H\}$ NMR study with **7′**, showed throughout the NMR experiment the presence of **7′**. This spectroscopic finding indicates that only a small percentage of **7′** enters the catalytic cycle. As a result, the GC–MS analysis of the NMR solution performed after the spectroscopic study confirmed a substrate conversion of only 10%.

The unique property of palladium–carbene complexes to be stable even in the presence of oxygen [18] stimulated us to carry out catalytic coupling reactions with **4b** in the presence of an optimized air pressure of 20 bar (Table 2, entries 14–19). The "in situ" generated Pd(OAc)$_2$(NEt$_3$)$_2$ precursor [7b] has been introduced as reference system for the aerobic oxidative alkyne coupling (Table 2, entries 30/31), performing only slightly better

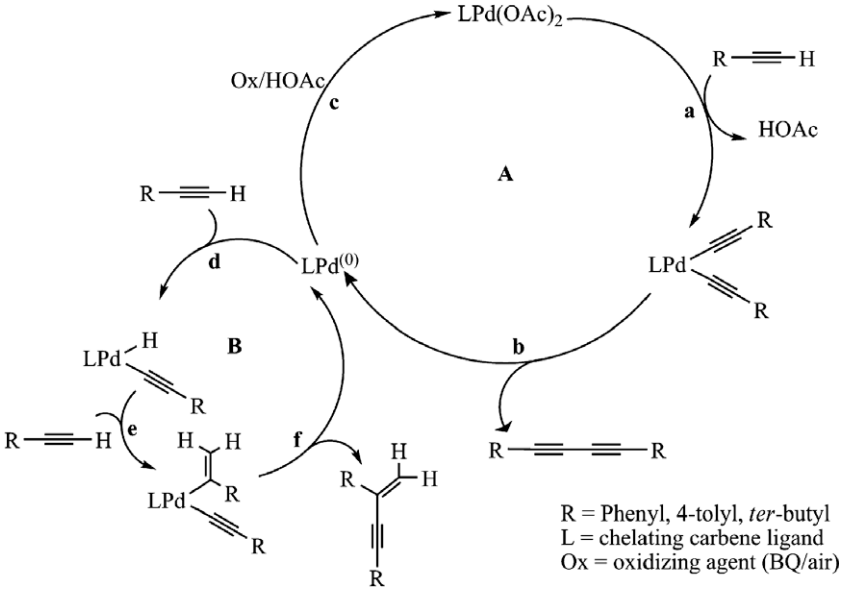

Scheme 5. Proposed catalytic cycles.

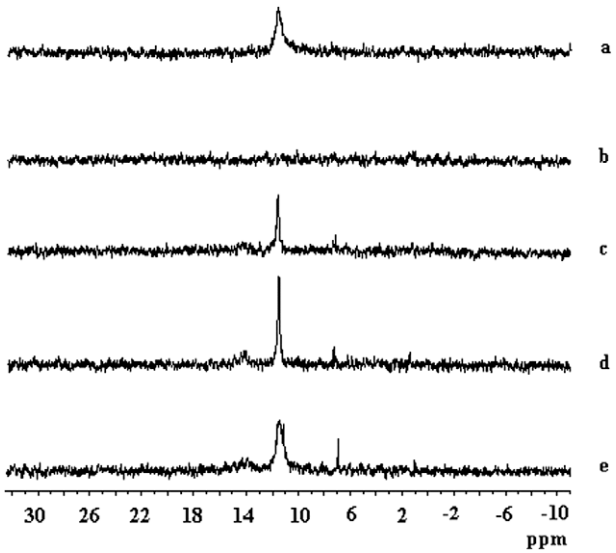

Fig. 9. Selected variable-temperature $^{31}P\{^1H\}$ NMR spectra (CD_3CN, 20–70 °C, 121.49 MHz) recorded during an oxidative coupling of phenylacetylene catalyzed by **6**: (a) solution of **6** (0.023 mmol) in CD_3CN (1.2 mL) at 20 °C; (b) after addition of phenylacetylene (0.546 mmol) and BQ (0.329 mmol) at 20 °C; (c) and (d) after heating the NMR solution to 50 and 70 °C, respectively; (e) after cooling the NMR solution to 20 °C.

than **4b** (entry 30 versus 14). In this context, it is worth mentioning that the latter precursor shows a good stability with time when air is used as oxidizing agent, regardless of the substrate employed (Table 2, entries 14–19). In fact, only a few efficient catalytic systems are known to use either oxygen or air as oxidizing agent for the oxidative coupling of terminal alkynes [7a–c,7j]. Furthermore, the only known copper-assisted palladium-NHC catalyzed aerobic alkyne coupling has been shown to be much less active as far as the coupling of phenylacethylene is concerned [13]. Regardless of the substrate used, catalytic reactions carried out in the presence of air gave significantly lower conversion compared to those performed in the presence of BQ. In fact, BQ is known to efficiently oxidize Pd^0 to Pd^{II} [19].

The two catalytic cycles as shown in Scheme 5 account for the coupling products observed in this study. Under oxidative catalytic conditions (i.e. in the presence of BQ or air) cycle A (Scheme 5) is operative yielding exclusively the 1,4-disubstituted 1,3-diyne as organic product. This latter catalytic cycle comprises the formation of a palladium bis-acetylide species [2a] (Scheme 5, step a), the reductive elimination of the coupling product under concomitant formation of a Pd^0 species (step b). This latter species then undergoes an acetic acid-assisted oxidative transformation into the precursor species (step c) closing in this way the catalytic cycle A. Evidence for the latter step has been provided by the variable-temperature $^{31}P\{^1H\}$ NMR study with **6** (vide supra), that showed unambiguously the reformation of the precursor species, once the substrate had been completely converted.

In the absence of an oxidizing agent the Pd^0 species enters the catalytic cycle B (Scheme 5), yielding the branched 1,3-enyne [10]. The experimental fact that 1,3-enynes are obtained along with a stoichiometric amount of the corresponding 1,3-diyne in the absence of an oxidizing agent is a prove for the interconnection of cycles A and B through a Pd^0 species.

3. Conclusions

A series of new palladium complexes with chelating (NHC) ligands have been prepared and completely characterized. The palladium acetate complexes have been employed as catalyst precursors for the copper-free oxidative homocoupling reactions of terminal alkynes to yield 1,4-substituted 1,3-diynes chemoselectively in the presence of BQ or air (20 bar). When BQ is used as oxidizing agent all catalysts studied herein experienced a significant deactivation process with time. Nevertheless, precursor **6** led to the highest substrate conversion, outperforming both reference systems (i.e. $Pd(OAc)_2$(dppe) and $Pd(OAc)_2$(dppp)). Within the series of the palladium bis-carbene precursors employed, compound **4b**, featured by *N*-1-naphthylenemethyl substituents at the imidazol-2-ylidine units and a bite angle of 88°, emerged as the most active precursor. Catalytic coupling reactions catalyzed by this compound in the presence of air, gave significantly lower substrate conversion compared to that performed in the presence of BQ. It also delivers slightly lower substrate conversion with respect to the reference system (i.e. $Pd(OAc)_2/NEt_3$). A variable-temperature

$^{31}P\{^1H\}$ NMR spectroscopic study with **6** carried out under oxidative homocoupling conditions (i.e. in the presence of BQ) proved the importance of the ancillary acetate ligands which close the catalytic cycle with an acetic acid-assisted reoxidation of a Pd^0 intermediate.

4. Experimental

4.1. Materials and instruments

All reactions were performed under a dry nitrogen atmosphere using standard Schlenk technique. All solvents used were purified according to standard procedures [20]. Commercially available chemicals were purchased from Aldrich or Acros. $Pd(OAc)_2$(dppe) [16a], $Pd(OAc)_2$(dppp) [16b], 1,1′-dibenzyl-3,3′-ethylenediimidazolium dichloride [12a], 1,1′-bis(1-naphthalenemethyl)-3,3′-ethylenediimidazolium dichloride [12a], **1a/b** [12a] and **5** [14] were prepared according to the literature procedure. ^1H, $^{13}C\{^1H\}$, $^{31}P\{^1H\}$ NMR spectra were recorded at 300.13, 75.48 and 121.49 MHz, respectively, on a Bruker AV-300 spectrometer. HMBC experiments were carried out with the same NMR spectrometer. Chemical shifts are reported in ppm (δ) relative to TMS, referenced to the chemical shifts of residual solvent resonances (^1H and $^{13}C\{^1H\}$ NMR) or 85% H_3PO_4 ($^{31}P\{^1H\}$ NMR). Elemental analyses were performed on a Heraeus CHN-OS Rapid elemental analyzer at the Instrument Center of National Chung Hsing University, Taiwan. Catalytic reactions were performed using a 320 mL stainless steel autoclave equipped with a mechanical stirrer and a Parr 4842 temperature and pressure controller. GC analyses of the catalytic solutions were performed with a Shimadzu GC-14A gas chromatograph equipped with a flame ionization detector and a SPB-1 Supelco fused silica capillary column (30 m, 0.25 mm i.d., 0.25 μm film thickness), using *n*-decane as internal standard. GC–MS analyses were performed on a Shimadzu QP2010S apparatus equipped with a column identical to that used for GC analysis. Conductivity measurements were carried out with an Orion model 990101 conductance cell connected to a model 101 conductivity meter. The conductivity data were obtained at a sample concentration of ca. 10^{-3} M solutions [21].

4.2. Synthesis

4.2.1. Synthesis of 1,1′-dibenzyl-3,3′-propylenediimidazolium dichloride

A mixture of 1-phenyl-1-ylmethyl-1*H*-imidazole (2.00 g, 12.60 mmol) and 1,3-dichloropropane (600 μL, 6.30 mmol) in THF (25 mL) was heated under reflux for 2 d. The solvent was then removed completely under vacuum. The residue was washed with dichloromethane (20 mL) obtaining a white solid that was filtered on a frit and dried under vacuum. Yield (0.81 g, 15%). Anal. Calc. for $C_{23}H_{26}Cl_2N_4$: C, 64.34; H, 6.10; N, 13.05. Found: C, 64.32; H, 5.86; N, 12.82%. ^1H NMR (300.13 MHz, DMSO-d_6, 294 K) (ppm): 2.50 (q, $^3J_{HH}$ = 7.0 Hz, 2H, $CH_2CH_2CH_2$), 4.37 (t, $^3J_{HH}$ = 7.0 Hz, 4H, NCH_2CH_2), 5.54 (s, 4H, $PhCH_2$), 7.34–7.38 (m, 6H, imi-H + Ph-H), 7.40–7.54 (m, 4H, Ph-H), 7.92–8.04 (m, 4H, Ph-H), 10.00 (s, 2H, NCHN); $^{13}C\{^1H\}$ NMR (75.48 MHz, DMSO-d_6, 294 K) (ppm): 29.74 (CCH_2C), 46.37 (NCH_2CH_2), 52.16 ($PhCH_2$), 122.86 imi-C), 123.16 (imi-C), 128.95 (Ph-C), 129.10 (Ph-C), 129.33 (Ph-C), 135.36 (Ph-C), 137.17 (NCN).

4.2.2. Synthesis of 1,1′-bis(1-naphthalenemethyl)-3,3′-propylenediimidazolium dichloride

A mixture of 1-naphthalen-1-ylmethyl-1*H*-imidazole (4.20 g, 20.0 mmol) and 1,3-dichloropropane (7.70 mL, 80.00 mmol) were heated under reflux for 2 d. The solvent was concentrated to about 15 mL under vacuum. Upon addition of dichloromethane (15 mL), a white solid was formed that was successively filtered on a frit and dried under vacuum. Yield (2.35 g, 22%). Anal. Calc. for $C_{31}H_{30}Cl_2N_4{\cdot}H_2O$: C, 68.00; H, 5.89; N, 10.23. Found C, 68.22; H, 6.16; N, 10.23%. ^1H NMR (300.13 MHz, DMSO-d_6, 294 K) (ppm): 2.46 (q, $^3J_{HH}$ = 7.0 Hz, 2H, $CH_2CH_2CH_2$), 4.31 (t, $^3J_{HH}$ = 7.0 Hz, 4H, NCH_2CH_2), 6.02 (s, 4H, $NpCH_2$), 7.53 (s, 2H, imi-H), 7.56–7.63 (m, 10H, imi-H, Np-H), 7.85 (s, 2H, Np-H), 8.00 (t, $^3J_{HH}$ = 7.5 Hz, 2H, Np-H), 8.25 (d, $^3J_{HH}$ = 8.0 Hz, 2H, Np-H), 9.81 (s, 2H, NCHN); $^{13}C\{^1H\}$ NMR (75.48 MHz, DMSO-d_6, 294 K) (ppm): 29.84 (CCH_2C), 46.39 (NCH_2CH_2), 50.14 ($NpCH_2$), 123.02 (imi-C), 123.17 (imi-C), 123.61, 126.07, 126.78, 127.60, 128.30, 129.24, 129.99, 130.66, 130.88, 133.80 (Np-C), 137.40 (NCN).

4.2.3. Synthesis of **2a**

A mixture of 1,1′-dibenzyl-3,3′-propylenediimidazolium dichloride (100.0 mg, 0.230 mmol) and $Pd(OAc)_2$ (52.0 mg, 0.230 mmol) in DMSO (5 mL) was heated at 50 °C for 3 h and then at 110 °C for 2 h. The solvent was then removed completely under vacuum. The residue was washed with THF (3 × 15 mL) obtaining a white solid that was filtered on a frit and then dried under vacuum. Yield (120.0 mg, 97%). Anal. Calc. for $C_{23}H_{24}N_4Cl_2Pd$: C, 51.75; H, 4.53; N, 10.50. Found: C, 51.22; H, 4.99; N, 9.94%. ^1H NMR (300.13 MHz, DMSO-d_6, 294 K) (ppm): 1.91 (m, 1H, $CH_2CH_aH_bCH_2$), 2.54 (m, 1H, $CH_2CH_aH_bCH_2$), 4.42 (m, 2H, $NCH_aH_bCH_2$), 4.97 (m, 2H, $NCH_aH_bCH_2$), 4.80 (d, $^2J_{HH}$ = 15.0 Hz, 2H, NCH_aH_bPh), 5.88 (d, $^2J_{HH}$ = 15.0 Hz, 2H, NCH_aH_bPh), 6.95 (s, 2H, imi-H), 7.23 (m, 4H, Ph-H), 7.35 (m, 8H, imi-H + Ph-H); $^{13}C\{^1H\}$ NMR (75.48 MHz, DMSO-d_6, 294 K) (ppm): 31.75 (CCH_2C), 51.99 (NCH_2CH_2), 53.27 ($PhCH_2$), 121.64 (imi-C), 124.35 (imi-C), 128.43, 129.42, 128.97, 136.67, 159.94 (NCN).

4.2.4. Synthesis of **2b**

The synthetic protocol is similar to that of **2a**. A mixture of 1,1′-bis(1-naphthalenemethyl)-3,3′-propylenediimidazolium dichloride (260.0 mg, 0.490 mmol) and $Pd(OAc)_2$ (110.0 mg, 0.490 mmol) was used. An off-white solid was obtained. Yield (299.0 mg, 96%). Anal. Calc. for $C_{31}H_{28}N_4Cl_2Pd$: C, 58.74; H, 4.45; N, 8.84. Found: C, 58.89; H, 4.35; N, 8.63. ^1H NMR (300.13 MHz, DMSO-d_6, 294 K) (ppm): 2.00 (m, 1H, $CH_2CH_aH_bCH_2$), 4.52 (m, 2H, $NCH_aH_bCH_2$), 5.06 (m, 2H, $NCH_aH_bCH_2$), 5.24 (d, $^2J_{HH}$ = 16.0 Hz, 2H, NCH_aH_bNp), 6.03 (d, $^2J_{HH}$ = 16.0 Hz, 2H, NCH_aH_bNp), 6.56 (d, $^3J_{HH}$ = 7.2 Hz, 2H, Np-H), 6.96 (s, 2H, imi-H), 7.62 (s, 2H, imi-H), 7.35 (t, $^3J_{HH}$ = 8.0 Hz, 2H, Np-H), 7.45–7.60 (m, 6H, Np-H), 7.92 (d, $^3J_{HH}$ = 8.0 Hz, 2H, Np-H), 8.01 (d, $^3J_{HH}$ = 8.0 Hz, 2H, Np-H). (The signal for $CH_2CH_aH_bCH_2$ was overlapped with the residual DMSO solvent peak at ca. 2.5 ppm.) $^{13}C\{^1H\}$ NMR (75.48 MHz, DMSO-d_6, 294 K) (ppm): 31.93 (CCH_2C), 51.19 (NCH_2CH_2), 52.21 ($NpCH_2$), 122.16, 123.20, 124.28, 125.23, 125.74, 126.05, 126.68, 127.22, 128.79, 130.48, 132.24, 133.49, 160.75 (NCN).

4.2.5. Synthesis of **3a**

Complex **1a** [12a] (104.0 mg, 0.200 mmol) was dissolved in dichloromethane (10 mL). Then AgOAc (73.0 mg, 0.440 mmol) was added and the mixture was stirred at room temperature for 3 h. The resulting suspension was filtered thought celite to remove AgCl and excess AgOAc. The solvent was then concentrated to a small volume (2 mL), followed by the addition of Et_2O (15 mL), affording a crude precipitate, which was recrystallized from DMF/Et_2O to give a pale yellow solid. Yield (294.0 mg, 52%). Anal. Calc. for $C_{26}H_{28}N_4O_4Pd$: C, 55.08; H, 4.98; N, 9.88. Found: C, 55.15; H, 4.86; N, 9.66%. ^1H NMR (300.13 MHz, DMSO-d_6, 294 K) (ppm): 1.58 (s, 6H, CH_3), 4.48–4.51 (m, 2H, $NCH_aH_bCH_2$), 5.20 (AB doublet, $^2J_{HH}$ = 15.0 Hz, 2H, CH_aH_bPh), 5.36 (AB doublet, $^2J_{HH}$ = 15.0 Hz, 2H, CH_aH_bPh), 5.46–5.48 (m, 2H, $NCH_aH_bCH_2$), 7.16 (s, 2H, imi-H), 7.23–7.38 (m, 12 H, Ph-H + imi-H); $^{13}C\{^1H\}$ NMR (75.48 MHz, DMSO-d_6, 294 K)

(ppm): 24.14 (CH_3), 47.02 (NCH_2CH_2), 52.39 (CH_2Ph), 121.73 (imi-C), 123.01 (imi-C), 127.75, 128.52, 137.03, 156.75 (NCN), 174.31 (CO). Crystals suitable for structural determination were obtained by vapor diffusion of diethyl ether into a dichloromethane solution of the compound.

4.2.6. Synthesis of **3b**

The synthetic protocol is similar to that of **3a**. Complex **1b** (124.0 mg, 0.200 mmol) and AgOAc (73.0 mg, 0.440 mmol) were used. After recrystallization of the crude product, a pale yellow solid was obtained. Yield (367.0 mg, 55%). Anal. Calc. for $C_{34}H_{32}N_4O_4Pd{\cdot}0.5H_2O$: C, 60.41; H, 4.92; N, 8.29. Found: C, 60.21; H, 5.11; N, 8.06%; ^{1}H NMR (300.13 MHz, DMSO-d_6, 294 K) (ppm): 1.47 (s, 6H, CH_3), 4.58–4.61 (m, 2H, $NCH_aH_bCH_2$), 5.53–5.71 (m, 6H, $CH_2Np + NCH_aH_bCH_2$), 6.67 (d, $^3J_{HH}$ = 7.0 Hz, 2H, Np-H), 7.16 (s, 2H, imi-H), 7.38–7.61 (m, 8H, imi-H + Np-H), 7.75 (d, $^3J_{HH}$ = 8.0 Hz, 2H, Np-H), 7.93 (d, $^3J_{HH}$ = 8.0 Hz, 2H, Np-H), 8.02 (d, $^3J_{HH}$ = 8.0 Hz, 2H, Np-H); ^{13}C{^{1}H} NMR (75.48 MHz, DMSO-d_6, 294 K) (ppm): 24.01 (CH_3), 47.09 (NCH_2CH_2), 50.49 (CH_2Ph), 122.13, 122.83, 122.94, 124.57, 125.50, 126.16, 126.62, 128.11, 128.65, 130.19, 132.56, 133.16, 158.01 (NCN), 174.30 (CO) ppm. Crystals suitable for structural determination were obtained by vapor diffusion of hexane into a DMF solution of the compound.

4.2.7. Synthesis of **4a**

The synthetic protocol is similar to that of **3a**. Complex **2a** (106.0 mg, 0.200 mmol) and AgOAc (73.0 mg, 0.440 mmol) were used. After recrystallization, an off-white solid was obtained. Yield (273.0 mg, 47%). Anal. Calc. for $C_{27}H_{30}N_4O_4Pd{\cdot}H_2O$: C, 54.13; H, 5.38; N, 9.36; Found: C, 54.62; H, 5.17; N, 9.10%; ^{1}H NMR (300.13 MHz, DMSO-d_6, 294 K) (ppm): 1.59 (s, 6H, CH_3), 1.78–1.97 (m, 1H, $CH_2CH_aH_bCH_2$), 2.25–2.43 (m, 1H, $CH_2CH_aH_bCH_2$), 4.26–4.29 (m, 2H, $NCH_aH_bCH_2$), 4.96 (d, $^3J_{HH}$ = 15.0 Hz, 2H, $PhCH_aH_b$), 5.54–5.62 (m, 2H, $NCH_aH_bCH_2$), 5.97 (d, $^2J_{HH}$ = 15.0 Hz, 2H, $PhCH_aH_b$), 6.99 (s, 2H, imi-H), 7.07 (s, 4H, imi-H + Ph-H), 7.33 (s, 8H, Ph-H); ^{13}C{^{1}H} NMR (75.48 MHz, DMSO-d_6, 294 K) (ppm): 24.04 (CH_3), 31.29 (CCH_2C), 51.33 (NCH_2CH_2), 52.79 ($PhCH_2$), 121.08 (imi-C), 124.00 (imi-C), 127.44, 127.80, 128.56, 136.93, 159.58 (NCN), 174.33 (CO) ppm. Crystals suitable for structural determination were obtained by vapor diffusion of diethyl ether into a dichloromethane solution of the compound.

4.2.8. Synthesis of **4b**

An analogous synthetic protocol used for the synthesis of **4a** was applied. Complex **2b** (127.0 mg, 0.200 mmol) and AgOAc (73.0 mg, 0.440 mmol) were used. After recrystallization of the crude product, a pale green solid was obtained. Yield (334.0 mg, 49%). Anal. Calc. for $C_{35}H_{34}N_4O_4Pd{\cdot}H_2O$: C, 60.13; H, 5.19; N, 8.01. Found: C, 59.90; H, 5.36; N, 7.89%. ^{1}H NMR (300.13 MHz, DMSO-d_6, 294 K) (ppm): 1.41 (s, 6H, CH_3), 1.88–2.11 (m, 1H, $CH_2CH_aH_bCH_2$), 4.37–4.40 (m, 2H, $NCH_aH_bCH_2$), 5.31 (d, $^2J_{HH}$ = 16.0 Hz, 2H, NCH_aH_bNp), 5.58 (m, 2H, $NCH_aH_bCH_2$), 5.86 (d, $^2J_{HH}$ = 16.0 Hz, 2H, NCH_aH_bNp), 6.11 (d, $^3J_{HH}$ = 7.0 Hz, 2H, Np-H), 7.01 (s, 2H, imi-H), 7.27–7.29 (m, 4H, Np-H), 7.46–7.51 (m, 4H, imi-H + Np-H), 7.65 (t, $^3J_{HH}$ = 7.0 Hz, 2H, Np-H), 7.86 (d, $^3J_{HH}$ = 8.0 Hz, 2H, Np-H), 8.01 (d, $^3J_{HH}$ = 8.0 Hz, 2H, Np-H); (The signal for $CH_2CH_aH_bCH_2$ was overlapped with the residual DMSO solvent peak at ca. 2.5 ppm.) ^{13}C{^{1}H} NMR (75.48 MHz, DMSO-d_6, 294 K) (ppm): 23.85 (CH_3), 31.46 (CCH_2C), 50.56 ($NpCH_2$), 51.51 (NCH_2CH_2), 121.82 (imi-C), 122.25, 122.77, 123.89 (imi-C), 125.36, 126.25, 126.72, 127.76, 128.66, 129.69, 132.84, 132.96 (Np-C), 160.70 (NCN), 174.07 (CO). Crystals suitable for structural determination were obtained by vapor diffusion of diethyl ether into a dichloromethane solution of the compound.

4.2.9. Synthesis of **6**

Compound **5** (979.0 mg, 1.370 mmol) was dissolved in a (3:1, v:v) solvent mixture (20 mL) of dichloromethane and acetonitrile. Silver acetate (479.0 mg, 2.870 mmol) was added and the mixture was then stirred in the dark for 6 h. The reaction mixture was then filtered through a plug of celite and the solvent of the filtrate was removed completely under vacuum. The residue was then washed with diethyl ether (2 × 25 mL) and the obtained pale yellow solid was filtered on a frit and dried under vacuum. Yield (673.0 mg, 85%). Anal. Calc. for $C_{27}H_{27}N_2O_4PPd{\cdot}0.5CHCl_3{\cdot}0.5H_2O$: C, 50.15; H, 4.51; N, 4.25. Found: C, 50.15; H, 4.51; N, 4.25%. ^{1}H NMR (300.13 MHz, $CDCl_3$, 294 K) (ppm): 1.37 (s, 3H, CH_3CO), 1.88 (s, 3H, CH_3CO), 3.33 (s, 3H, NCH_3), 4.91 (d, $^2J_{HH}$ = 15.3 Hz, 1H, NCH_aH_b), 6.46 (s, 1H, imi-H), 6.85–6.89 (m, 2H, NCH_aH_b, imi-H), 7.22–7.64 (m, 14H, Ar-H); ^{13}C{^{1}H} NMR (75.48 MHz, $CDCl_3$, 294 K) (ppm): 22.9 (CH_3CO), 35.8 (CH_3CO), 40.8 (NCH_3), 53.8 (d, $^3J_{PC}$ = 6.6 Hz, CH_2), 120.8 (imi-C), 123.5 (imi-C), 126.8, (d, $^1J_{PC}$ = 50.7 Hz, Ar–C), 127.9 (d, $^2J_{PC}$ = 11.5 Hz, Ar-C), 128.5 (d, $^2J_{PC}$ = 11.4 Hz, Ar-C), 128.4–129.1 (overlapping signals, Ar-C), 129.4 (s, Ar-C), 130.4 (d, $^3J_{PC}$ = 2.6 Hz, Ar-C), 130.6 (d, $^2J_{PC}$ = 8.8 Hz, Ar-C), 130.9 (d, $^3J_{PC}$ = 2.4 Hz, Ar-C), 132.1 (d, $^3J_{PC}$ = 2.0 Hz, Ar-C), 132.8 (d, $^2J_{PC}$ = 11.9 Hz, Ar-C), 133.2 (d, $^2J_{PC}$ = 11.0 Hz, Ar-C), 137.4 (d, $^3J_{PC}$ = 2.2 Hz, Ar-C), 141.6 (d, $^2J_{PC}$ = 11.4 Hz, Ar–C), 154.3 (d, $^2J_{PC}$ = 11.6 Hz, NCN), 176.8 (CO), 177.4 (CO); ^{31}P{^{1}H} NMR (121.49 MHz, $CDCl_3$, 294 K) (ppm): 12.5 (s). Crystals suitable for structural determination were obtained by evaporating a chloroform solution of the compound.

4.2.10. Synthesis of **7** and **7′**

Compound **6** (120.0 mg, 0.207 mmol) was dissolved in a deaerated (1:1, v:v) solvent mixture (10 mL) of dichloromethane and methanol. To this solution was added solid *p*-TsOH (82.6 mg, 0.435 mmol) under vigorous stirring at room temperature. After a reaction time of half an hour, the solution was concentrated to a small volume (3 mL) and upon a slow addition of diethyl ether (10 mL) **7** was obtained as yellow micro-crystalline solid. Yield (25.0 mg, 75%). Anal. Calc. for $C_{37}H_{35}N_2O_6PS_2Pd$: C, 55.21; H, 4.35; N, 3.48. Found: C, 55.12; H, 4.27; N, 3.34%; ^{1}H NMR (300.13 MHz, CD_2Cl_2, 294 K) (ppm): 2.36 (s, 6H, $ArCH_3$), 3.39 (s, 3H, NCH_3), 5.21 (d, $^2J_{HH}$ = 15.6 Hz, 1H, NCH_aH_b), 6.71 (s, 1H, $^3J_{HH}$ = 1.9 Hz, imi-H), 6.89 (m, 1H, 1H, imi-H), 6.99 (d, $^2J_{HH}$ = 15.6 Hz, 1H, NCH_aH_b), 7.09 (d, $^3J_{HH}$ = 7.8 Hz, 4H, Ar-H(tosylate)), 7.27–7.51 (m, 13H, Ar-H), 7.52 (d, $^3J_{HH}$ = 7.8 Hz, 4H, Ar-H(tosylate)), 7.68 (t, $^3J_{HH}$ = 7.1 Hz, 1H, Ar-H); ^{13}C{^{1}H} NMR (75.48 MHz, CD_2Cl_2, 294 K) (ppm): 21.06 (s, $ArCH_3$), 36.54 (s, NCH_3), 53.20 (s, NCH_aH_b, overlapped signal), 122.48 (s, imi-C), 125.21 (s, Ar-C), 125.30 (d, $^1J_{PC}$ = 57.6 Hz, Ar-C), 126.09 (s, Ar-C(tosylate)), 126.80 (d, $^1J_{PC}$ = 57.6 Hz, Ar-C), 127.90 (d, $^1J_{PC}$ = 62.5 Hz, Ar-C), 128.60 (s, Ar-C(tosylate)), 129.20 (d, $^2J_{PC}$ = 11.1 Hz, Ar-C), 131.05 (d, $^2J_{PC}$ = 8.8 Hz, Ar-C), 131.77 (d, $^2J_{PC}$ = 10.1 Hz, Ar-C), 132.60 (d, $^2J_{PC}$ = 11.1 Hz, Ar-C), 132.91 (s, Ar-C(tosylate)), 133.98 (d, $^2J_{PC}$ = 11.1 Hz, Ar-C), 136.96 (s, Ar-C), 140.35 (s, Ar-C(tosylate)), 141.80 (d, $^2J_{PC}$ = 10.5 Hz, Ar-C), 141.36 (s, Ar-C), 144.20 (d, $^2J_{PC}$ = 12.6 Hz, NCN); ^{31}P{^{1}H} NMR (121.49 MHz, CD_2Cl_2, 294 K) (ppm): 11.73 (s).

The dissolution of **7** in acetonitrile gives the bis cationic species **7′** (Scheme 3) which is stable only in the presence of the latter solvent. Selected NMR data for **7′**: ^{1}H NMR (300.13 MHz, CD_3CN, 294 K) (ppm): 2.33 (s, 6H, $ArCH_3$), 3.15 (s, 3H, NCH_3), 5.24 (d, $^2J_{HH}$ = 15.6 Hz, 1H, NCH_aH_b), 6.62 (d, $^2J_{HH}$ = 15.6 Hz, 1H, NCH_aH_b), 6.77 (d, $^3J_{HH}$ = 1.9 Hz, 1H, imi-H), 7.02 (m, 1H, Ar-H), 7.16 (d, $^3J_{HH}$ = 7.8 Hz, 4H, Ar-H(tosylate)), 7.29 (d, $^3J_{HH}$ = 1.9 Hz, 1H, imi-H), 7.31–7.77 (m, 17H, Ar-H + Ar-H(tosylate)); ^{31}P{^{1}H} NMR (121.49 MHz, CD_3CN, 294 K) (ppm): 10.62 (s); Λ_M (CH_3CN, 295 K): 150 Ω^{-1} cm^2 mol^{-1}.

4.3. Catalytic reactions in acetonitrile

The catalytic reactions were performed in a stainless steel autoclave (320 mL). The amount of precursor (0.02 mmol) and of BQ (2.30 mmol), if employed, was put in the autoclave, followed by its evacuation by means of a vacuum pump. Then a deaerated acetonitrile solution (25 mL) of the substrate (6.00 mmol) and *n*-decane (0.70 mmol, internal standard) was introduced into an evacuated autoclave by suction. The autoclave was then successively heated to 70 °C, mechanically stirred and charged with air pressure, if employed. After the desired reaction time, the autoclave was cooled to 6 °C by means of a water-ice bath, followed by the slow release of the air pressure, if present. Afterwards the catalytic solution was subjected to GC analysis in order to quantify the substrate conversion and to a GC/MS analysis to identify the obtained organic product.

4.4. Variable-temperature NMR study with compounds **6** and **7′** in CD_3CN

Since the variable-temperature NMR experiments with **6** and **7′** have been carried out analogously, the experimental procedure will be reported only for **6**. Precursor **6** (13.3 mg, 0.023 mmol) was dissolved in deareated CD_3CN (1.2 mL). The solution was then transferred into a 5 mm NMR tube under a nitrogen atmosphere. The NMR tube was then inserted into the NMR probe at room temperature followed by the acquisition of a $^{31}P\{^1H\}$ and a ^1H NMR spectrum. The NMR tube was then removed from the NMR probe and phenylacethylene (59.9 μL, 0.546 mmol) and BQ (35.5 mg, 0.329 mmol) were added to the solution under nitrogen. The sealed NMR tube was then again placed into the NMR probe, followed by the acquisition of a $^{31}P\{^1H\}$ and ^1H NMR spectrum. The NMR probe was then successively heated to 50 °C and to 70 °C, acquiring $^{31}P\{^1H\}$ and ^1H NMR spectra at both latter temperatures. After the acquisition of the last NMR spectrum at 70 °C, the probe was cooled to room temperature followed by the acquisition of a $^{31}P\{^1H\}$ and ^1H NMR spectrum. The NMR tube was then removed from the probe and the NMR solution was subjected to a GC/MS analysis.

In a separate NMR experiment, a CD_3CN solution (1.2 mL) of **6** (13.3 mg, 0.023 mmol), BQ (35.5 mg, 0.329 mmol) and phenylacethylene (59.9 μL, 0.546 mmol) was transferred into a 5 mm NMR tube, which was sealed and inserted into a pre-cooled (i.e. −40 °C) NMR probe. Both $^{31}P\{^1H\}$ and ^1H NMR spectra were acquired at the latter temperature.

4.5. X-ray crystallographic data collection and refinement of the structures

The crystallographic data for **1b**·DMF, **2b**·2DMF, **3a**, **3b**·DMF, **4a**, **4b** and **6**·$CHCl_3$·$2H_2O$ are summarized in Table 3.

Typically, the crystals were removed from the vial with a small amount of mother liquor and immediately coated with paratone–N oil on a glass slide. A suitable crystal was mounted on a glass fiber with silicone grease and placed in the cold stream of a Bruker APEX II equipped with as CCD area detector and a graphite monochromater utilizing Mo Kα radiation (λ = 0.71073 Å) at 150(2) K. The data were corrected for Lorentz and polarization effects using the Bruker SAINT software and an absorption correction was performed using the SADABS program [22a].

All structures were solved by direct methods using SHELXS-97 and refined by full-matrix least squares methods against F^2 with SHELXTL software package [22b]. All non-H atoms were refined anisotropically; H-atoms, except those of water in **6**, were fixed

Table 3
Crystallographic data and structure refinement details for **1b**·DMF, **2b**·2DMF, **3a**, **3b**·DMF, **4a**, **4b**, **6**·$CHCl_3$·$2H_2O$.

	1b·DMF	**2b**·2DMF	**3a**	**3b**·DMF	**4a**	**4b**	**6**·$CHCl_3$·$2H_2O$
Formula	$C_{33}H_{33}Cl_2N_5OPd$	$C_{37}H_{42}Cl_2N_6O_2Pd$	$C_{26}H_{28}N_4O_4Pd$	$C_{37}H_{39}N_5O_5Pd$	$C_{27}H_{30}N_4O_4Pd$	$C_{35}H_{34}N_4O_4Pd$	$C_{28}H_{32}Cl_3N_2O_6PPd$
Formula weight (g mol^{-1})	692.94	780.07	566.92	740.13	580.95	681.06	736.28
Crystal color, shape	Colorless, prism	Colorless, prism	Colorless, prism	Colorless, prism	Colorless, prism	Colorless, prism	Yellow, block
Crystal size (mm)	0.45 × 0.2 × 0.16	0.26 × 0.11 × 0.08	0.42 × 0.17 × 0.15	0.23 × 0.22 × 0.13	0.24 × 0.17 × 0.17	0.42 × 0.29 × 0.29	0.34 × 0.20 × 0.13
T (K)	150	150	150	150	150	150	150
Crystal system	Monoclinic	Triclinic	Triclinic	Monoclinic	Triclinic	Orthorhomic	Triclinic
Space group	$P2_1/c$	$P\bar{1}$	$P\bar{1}$	$P2_1/n$	$P\bar{1}$	$P2_12_12_1$	$P\bar{1}$
a (Å)	10.3247(16)	11.6846(4)	9.3140(6)	16.0340(8)	9.9334(2)	10.7858(4)	8.6653(5)
b (Å)	19.505(3)	11.6879(4)	16.3364(11)	10.7180(5)	13.7586(3)	16.0185(5)	16.1527(9)
c (Å)	14.986(2)	14.2139(5)	18.0377(13)	21.0621(10)	19.2167(4)	21.0902(8)	23.1016(13)
α (°)	90	105.922(2)	115.650(3)	90	79.1680(10)	90	97.428(1)
β (°)	96.854(3)	104.137(2)	92.325(3)	108.6780(10)	87.269(2)	90	91.899(1)
γ (°)	90	96.465(2)	91.473(3)	90	89.7240(10)	90	99.639(1)
V (Å^3)	2996.4(8)	1776.27(11)	2469.2(3)	3428.9(3)	2576.59(9)	3643.8(2)	3156.1(3)
Z	4	2	4	4	4	4	4
Density (calculated) (g cm^{-3})	1.536	1.458	1.525	1.434	1.498	1.241	1.550
F(0 0 0)	1.416	804	1160	1528	1192	1400	1496
θ Range (°)	1.72-27.52	1.83-28.31	1.25-27.00	1.93-28.68	1.51-28.74	1.93-28.73	1.46-27.00
μ (mm^{-1})	0.834	0.715	0.791	0.591	0.760	0.548	0.935
Measured reflections	29 796	20 721	31 014	39 692	37 990	24 962	37 003
Independent reflections	6868	8776	10 656	8834	13 312	9399	13 595
Data/restraints/parameters	6828/0/379	8776/0/437	10 656/126/668	8834/0/437	13 312/0/652	9399/0/399	13 595/1/745
Goodness-of-fit on F^2	0.918	1.028	0.979	1.005	0.987	0.895	1.043
R_1, wR_2 [$I > 2\sigma I$)]	0.0318, 0.0730	0.0376, 0.0767	0.0565, 0.1361	0.0392, 0.0819	0.0436, 0.0869	0.0566, 0.1131	0.0315, 0.0890
R_1, wR_2 (all data)	0.0466, 0.0774	0.0590, 0.0820	0.1100, 0.1599	0.0751, 0.0922	0.0897, 0.0991	0.1105, 0.1274	0.0427, 0.0938
Largest difference peak/hole (e Å^{-3})	1.094/−0.368	0.464/−0.414	2.200/−1.111	0.500/−0.561	0.788/−0.642	0.871/−1.354	0.986/−0.679

at calculated positions and refined with the use of a riding model. The H-atoms of water in **6** were located from the difference map, but were not refined. One of the phenyl rings in **3a** is disordered but readily modeled. The diethyl ether and water molecules in **4b** are disordered and all attempts to model them failed. SQUEEZE function of the program PLATON was used to remove the solvent contribution from the intensity data and the structure was refined against a solvent-free model [22c].

5. Supplementary material

CCDC 230175, 720982,720983, 720985, 720984, 722178 and 722179 contain the supplementary crystallographic data for **1b**·DMF, **2b**·2DMF, **3a**, **3b**·DMF, **4a**, **4b**, **6**·$CHCl_3$·$2H_2O$. These data can be obtained free of charge from The Cambridge Crystallographic Data Centre via www.ccdc.cam.ac.uk/data_request/cif.

Acknowledgements

This work was financially supported by the Italy-Taiwan Bilateral Cooperation Project (NSC 97-2923-M-018-001-MY2). Thanks are also given to the European Commission for financing the project IDECAT (NoE Contract No. NMP3-CT-2005-011730).

References

[1] (a) A.B. Holmes, C.L.D. Jennings-White, D.A. Kendrick, J. Chem. Soc., Chem. Commun. (1983) 415–417;
(b) A. Stütz, Angew. Chem., Int. Ed. Engl. 26 (1987) 320–328;
(c) T.R. Hoye, P.R. Hanson, Tetrahedron Lett. 34 (1993) 5043–5046.
[2] (a) R.E. Martin, F. Diederich, Angew. Chem., Int. Ed. 38 (1999) 1350–1377;
(b) J.M. Tour, Chem. Rev. 96 (1996) 537–553;
(c) N.C. Greenham, S.C. Moratti, D.D.C. Bradley, R.H. Friend, A.B. Holmes, Nature 365 (1993) 628–630;
(d) R.E. Martin, T. Mäder, F. Diederich, Angew. Chem., Int. Ed. 38 (1999) 817–821.
[3] P. Siemsen, R.C. Livingston, F. Diederich, Angew. Chem., Int. Ed. 39 (2000) 2632–2657.
[4] L. Fomina, B. Vazquez, E. Tkatchouk, S. Fomine, Tetrahedron 58 (2002) 6741–6747.
[5] A.S. Hay, J. Org. Chem. 27 (1962) 3320–3321.
[6] K. Kamata, S. Yamaguchi, M. Kotani, K. Yamaguchi, N. Mizuno, Angew. Chem., Int. Ed. 47 (2008) 2407–2410.
[7] (a) A.S. Batsanov, J.C. Collings, I.J.S. Fairlamb, J.P. Holland, J.A.K. Howard, Z. Lin, T.B. Marder, A.C. Parsons, R.M. Ward, J. Zhu, J. Org. Chem. 70 (2005) 703–706;
(b) J.-H. Li, Y. Liang, Y.-X. Xie, J. Org. Chem. 70 (2005) 4393–4396;
(c) C. Ye, J.-Cj. Xiao, B. Twamley, A.D. LaLonde, M.G. Norton, J.M. Shreeve, Eur. J. Org. Chem. (2007) 5095–5100;
(d) M. Vlassa, I. Ciocan-Tarta, F. Mărgineanu, I. Oprean, Tetrahedron 52 (1996) 1337–1342;
(e) Q. Liu, D.J. Burton, Tetrahedron Lett. 38 (1997) 4371–4374;
(f) A. Lei, M. Srivastava, X. Zhang, J. Org. Chem. 67 (2002) 1969–1971;
(g) J.-H. Li, Y. Liang, X.-D. Zhang, Tetrahedron 61 (2005) 1903–1907;
(h) R. Rossi, A. Carpita, C. Bigelli, Tetrahedron Lett. 26 (1985) 523–526;
(i) I.J.S. Fairlamb, P.S. Bäuerlein, L.R. Marrison, J.M. Dickinson, Chem. Commun. (2003) 632–633;
(j) E. Valenti, M.A. Pericàs, F. Serratosa, J. Am. Chem. Soc. 112 (1990) 7405–7406.
[8] (a) S.V. Damle, D. Seomoon, P.H. Lee, J. Org. Chem. 68 (2003) 7085–7087;
(b) C.H. Oh, V.R. Reddy, Tetrahedron Lett. 45 (2004) 5221–5224.
[9] (a) K. Osakada, M. Hamada, T. Yamamoto, Organometallics 19 (2000) 458–468;
(b) A.L. Sadowy, M.J. Ferguson, R. McDonald, R.R. Tykwinski, Organometallics 27 (2008) 6321–6325;
(c) A. Sebald, C. Stader, B. Wrackmeyer, J. Organomet. Chem. 311 (1986) 233–242.
[10] (a) B.M. Trost, M.T. Sorum, C. Chan, A.E. Harms, G. Rühter, J. Am. Chem. Soc. 119 (1997) 698–708;
(b) B.M. Trost, C. Chan, G. Ruther, J. Am. Chem. Soc. 109 (1987) 3486–3487.
[11] (a) W.A. Herrmann, C.-P. Reisinger, M. Spiegler, J. Organomet. Chem. 557 (1998) 93–96;
(b) M.G. Gardiner, W.A. Herrmann, C.-P. Reisinger, J. Schwarz, M. Spiegler, J. Organomet. Chem. 572 (1999) 239–247;
(c) S. Ahrens, A. Zeller, M. Taige, T. Strassner, Organometallics 25 (2006) 5409–5415;
(d) T.A.P. Paulose, J.A. Olson, J.W. Quail, S.R. Foley, J. Organomet. Chem. 693 (2008) 3405–3410;
(e) R.E. Douthwaite, M.L.H. Green, P.J. Silcock, P.T. Gomes, J. Chem. Soc., Dalton Trans. (2002) 1386–1390;
(f) M. Muehlhofer, T. Strassner, W.A. Herrmann, Angew. Chem., Int. Ed. 41 (2002) 1745–1747;
(g) H.V. Huynh, D. Le Van, F.E. Hahn, T.S.A. Hor, J. Organomet. Chem. 689 (2004) 1766–1770;
(h) J.C. Slootweg, P. Chen, Organometallics 25 (2006) 5863–5869;
(i) T. Strassner, M. Muehlhofer, A. Zeller, E. Herdtweck, W.A. Herrmann, J. Organomet. Chem. 689 (2004) 1418–1424;
(j) M.A. Taige, A. Zeller, S. Ahrens, S. Goutal, E. Herdtweck, T. Strassner, J. Organomet. Chem. 692 (2007) 1519–1529;
(k) S.K. Schneider, J. Schwarz, G.D. Frey, E. Herdtweck, W.A. Herrmann, J. Organomet. Chem. 692 (2007) 4560–4568.
[12] (a) H.M. Lee, C.Y. Lu, C.Y. Chen, W.L. Chen, H.C. Lin, P.L. Chiu, P.Y. Cheng, Tetrahedron 60 (2004) 5807–5828;
(b) P.L. Chiu, C.Y. Chen, J.Y. Zeng, C.Y. Lu, H.M. Lee, J. Organomet. Chem. 690 (2005) 1682–1687;
(c) H.M. Lee, P.L. Chiu, Acta Crystallogr., Sect. E 60 (2004) m1276–1277.
[13] M. Shi, H. -xin Qian, Appl. Organomet. Chem. 20 (2006) 771–774.
[14] C.-C. Ho, S. Chatterjee, T.-L. Wu, Y.-W. Chang, K.-T. Chan, T.-H. Hsiao, H.M. Lee, Organometallics 28 (2009) 2837–2847.
[15] J.A. Mata, A.R. Chianese, J.R. Miecznikowski, M. Poyatos, E. Peris, J.W. Faller, R.H. Crabtree, Organometallics 23 (2004) 1253–1263.
[16] (a) C. Bianchini, H.M. Lee, A. Meli, W. Oberhauser, M. Peruzzini, F. Vizza, Organometallics 21 (2002) 16–33;
(b) B. Milani, L. Vicentini, A. Sommazzi, F. Garbassi, E. Chiarparin, E. Zangrando, G. Mestroni, J. Chem. Soc., Dalton Trans. (1996) 3139–3144.
[17] (a) Z. Freixa, P.W.N.M. van Leeuwen, Dalton Trans. (2003) 1890–1901;
(b) P. Dierkes, P.W.N.M. van Leeuwen, J. Chem. Soc., Dalton Trans. (1999) 1519–1529;
(c) M.J. Calhorda, J.M. Brown, N.A. Cooley, Organometallics 10 (1991) 1431–1438;
(d) T. Hayashi, M. Konishi, Y. Kobori, M. Kumada, T. Higuchi, K. Hirotsu, J. Am. Chem. Soc. 106 (1984) 158–163;
(e) J.E. Marcone, K.G. Moloy, J. Am. Chem. Soc. 120 (1998) 8527–8528;
(f) M.S. Driver, J.F. Hartwig, J. Am. Chem. Soc. 118 (1996) 7217–7218.
[18] (a) S.S. Stahl, Angew. Chem., Int. Ed. 43 (2004) 3400–3420;
(b) D.R. Jensen, M.J. Schultz, J.A. Mueller, M.S. Sigman, Angew. Chem., Int. Ed. 42 (2003) 3810–3813;
(c) M.J. Schultz, St.S. Hamilton, D.R. Jensen, M.S. Sigman, J. Org. Chem. 70 (2005) 3343–3352.
[19] E. Drent, P.H.M. Budzelaar, Chem. Rev. 96 (1996) 663–681.
[20] W.L.F. Armarego, C.L.L. Chai, Purification of Laboratory Chemicals, fifth ed., Elsevier Science, Burlington, 2003.
[21] (a) C. Bianchini, A. Meli, W. Oberhauser, A.M. Segarra, C. Claver, E.J. Garcia Suarez, J. Mol. Catal. A: Chem. 265 (2007) 292–305;
(b) C. Bianchini, A. Meli, W. Oberhauser, S. Parisel, E. Passaglia, F. Ciardelli, O.V. Gusev, A.M. Kal'sin, N.V. Vologdin, Organometallics 24 (2005) 1018–1030.
[22] (a) G.M. Sheldrick, SADABS, Bruker AXS Inc., Madison, WI, USA, 2001;
(b) G.M. Sheldrick, Acta Crystallogr., Sect. A 64 (2008) 112–122;
(c) A.L. Spek, J. Appl. Crystallogr. 36 (2003) 7–13.